# Particle surface area dependence of mineral dust in the immersion freezing mode: Investigations with freely suspended drops in an acoustic levitator and a vertical wind tunnel

**K. Diehl[1], M. Debertshäuser[1], O. Eppers[1], H. Schmithüsen[1], S.K. Mitra[1], and S. Borrmann[2]**

[1]{Institute of Atmospheric Physics, University of Mainz, Germany}

[2]{Max Planck Institute for Chemistry, Mainz, Germany}

Correspondence to: K. Diehl (kdiehl@uni-mainz.de)

## Abstract

The heterogeneous freezing temperatures of supercooled drops were measured using an acoustic levitator. This technique allows to freely suspend single drops in air without any wall contacts. Heterogeneous nucleation by two types of illite (illite IMt1 and illite NX) and a montmorillonite sample was investigated in the immersion mode. Drops of 1 mm in radius were monitored by a video camera while cooling down to -28°C to simulate freezing within the tropospheric temperature range. The surface temperature of the drops was contact-free determined with an infra-red thermometer; the onset of freezing was indicated by a sudden increase of the drop surface temperature. For comparisons, measurements with one particle type (illite NX) were additionally performed in the Mainz vertical wind tunnel with drops of 340 µm radius freely suspended. Immersion freezing was observed in a temperature range between -13 and -26°C as a function of particle type and particle surface area immersed in the drops. Isothermal experiments at the wind tunnel indicated that after the cooling stage freezing still proceeds at least during the investigated time period of 30 s. The results were evaluated by applying two descriptions of heterogeneous freezing, the stochastic and the singular model. Although the wind tunnel results do not support a time-independence of the

freezing process both models are applicable to compare the results from the two experimental techniques.

## 1 Introduction

The types and quantities of atmospheric ice nuclei affect ice cloud microphysical and radiative properties as well as their precipitation efficiency. This has been shown by modeling studies, e.g., Phillips et al. (2007), Storelvmo et al. (2008), and Hoose et al. (2008). The role of mineral dust particles as ice nuclei is undoubted (e.g., Hoose and Möhler, 2012). The most abundant minerals occurring in desert aerosols are quartz, calcite, mica, hematite, illite, and gypsum (Kandler et al., 2007). So far, laboratory experiments of heterogeneous freezing have been performed mainly with kaolinite, montmorillonite, and illite (e.g., Hoffer, 1961; Pitter and Pruppacher, 1973; Murray et al., 2011; Pinti et al., 2012, Broadley et al., 2012), and Arizona test dust or several types of natural dust (e.g., Vali, 2008; Connolly et al., 2009; Niedermeier et al., 2011; Kanji et al., 2011; Niemand et al., 2012).

To investigate drop freezing in the immersion mode, various experimental techniques are available; see the review paper of Hoose and Möhler (2012). These are, for instance, drop freezing devices with cooled surfaces (e.g., Zuberi et al., 2002; Knopf et al., 2011), emulsified drop freezing (e.g., Hoffer, 1961; Marcolli et al., 2007; Pummer et al., 2012), flow tubes (e.g., Niedermeier et al., 2011), continuous flow diffusion chambers (e.g., DeMott et al., 1999; Lüönd et al., 2010), cloud chambers (e.g., Connolly et al., 2009; Niemand et al., 2012), falling droplet chambers (Ladino et al., 2011), acoustic drop levitators (e.g., Ettner et al., 2004; Diehl et al., 2009), vertical wind tunnels (e.g., Pitter and Pruppacher, 1973; Diehl et al., 2002), and, for homogeneous freezing, electrodynamical drop levitators (e.g., Duft and Leisner, 2004).

The present experiments were performed with two techniques: the Mainz vertical wind tunnel where drops are freely suspended in air at their terminal velocities during freezing, and an acoustic drop levitator where contact-free levitation is achieved at the nodes of a standing ultrasonic wave. The advantage over measurements in a vertical wind tunnel is that the drops can be levitated for long time periods and are very still which allows direct determination of the surface temperature of the drops during the entire freezing process. Furthermore, it does not require a large air flow which makes it much more economical in its operation. On the other hand, in the wind tunnel, the drops reach equilibrium with the ambient temperature

within 3 to 5 seconds and, afterwards, can be kept at a constant temperature during observation. This allows to investigate any time dependencies of freezing processes.

The majority of the present experiments with the acoustic levitator were performed with two types of illite particles, illite IMt1 and illite NX, some studies were undertaken with montmorillonite. For comparisons, measurements with one particle type (illite NX) were additionally performed in the Mainz vertical wind tunnel. Two models were applied to interpret the results, the time-dependant stochastic model based on classical nucleation theory and the singular model which neglects time dependence in comparison to particle variability. Although the latter assumption is not valid in comparison to experimental observations (e.g., Murray et al., 2011; Broadley et al., 2012), the advantage of the singular model is that it allows to simplify the description of ice formation in cloud models (Vali, 2008).

The present investigations are part of the German research group INUIT (**I**ce **N**uclei research **U**n**IT**) which was established to study heterogeneous ice formation in the atmosphere. In laboratory experiments the nature of different ice nucleation processes and the chemical and microphysical characteristics of atmospherically relevant ice nuclei are investigated. An important issue of INUIT is that defined test aerosols which are distributed to the research groups are investigated with several experimental techniques and the results are compared. Parameterizations based on these common experiments will be fed into cloud models to simulate mixed-phase cloud microphysics and to quantify the contribution of ice nuclei types and freezing modes. For more details see the INUIT website: www.ice-nuclei.de.

## 2 Experimental details

### 2.1 Acoustic levitator

The acoustic levitator was also used in two earlier studies of the homogenous freezing of supercooled binary and ternary solution drops (Ettner et al.; 2004; Diehl et al.; 2009). The results indicated that the Koop formulation based on the water activity (Koop et al., 2000) is valid as well for large drop sizes as used in the acoustic levitator. During the present experiments, the acoustic levitator was installed inside a walk-in cold chamber which achieves ambient temperatures down to -35°C. These are sufficient for heterogeneous freezing of water drops. As an improvement to the earlier experiments, an infra-red thermometer was used to determine the drop surface temperature.

### 2.1.1 Instruments and data acquisition

The employed acoustic levitator is the type APOS BA 10 from the company TEC5 as shown in Figure 1 (picture included on the left side). Inside the trap an ultrasonic wave is produced by a piezoelectric oscillator and reflected by a concave Teflon reflector plate. The interference generates a standing wave with five nodes between the oscillator and the reflector. The oscillator is powered by a special HF-oscillator power supply. It operates at a fixed frequency of 58 kHz and has an electrical output power of 0.6 to 5W which is regulated by a potentiometer. While the source is fixed the reflector is movable mounted on a micrometer screw. In this way the distance between the source and the reflector can be varied by several millimetres to achieve optimal reflector separation at the operating frequency and temperature. Also, optimally, at the third of the five existing nodes drops with diameters between 100 µm and 3 mm can be levitated. The trap was surrounded by an acrylic glass cylinder to protect the levitated drops from the outside air motions of the walk-in cold chamber in order to establish stable temperature conditions during the experiments.

The set-up in the cold chamber (see Figure 1) includes the acoustic levitator, a platinum-resistor thermometer Pt100, a digital video camera (FireWire-CAM-011H from Phytec), and an infra-red thermometer (KT 19.82 II from Heitronics). The video camera and the infra-red thermometer were mounted on adjustable laboratory stages and arranged around the levitator on sliding rails so that their height and distance to the suspended drop could be adjusted. The video camera allowed a visual observation of the freezing process. The infra-red thermometer was used to measure the surface temperature of the freezing drops with an accuracy of 0.7K while the Pt100 sensor was located in the vicinity of the drop to measure the ambient temperature. Before each series of experiments the infra-red thermometer was calibrated by use of the Pt100 as reference. For the calibration the Pt100 was coated with a layer of water by dipping it in water which subsequently froze below 0°C. The infrared thermometer translates the incoming radiation into temperature reading making an implicit assumption of the radiating surface. Therefore, the ceramic surface of the Pt100 sensor had to be coated with a thin layer of ice to represent the freezing drop surface emissivity in a more realistic way. The advantage of the acoustic levitator is that the drops are held stationary with a high positional precision. Of course this is not the case for atmospheric drops, however, freezing as a hydrodynamical process should not be affected. When the ultra-sonic field is kept well isolated from ambient air disturbances, no drop movements are visible with the naked eye.

This allows performing direct and contact-free temperature measurements of the drop surface during the entire freezing process. As the area of surface temperature observation is a circular spot of approximately 1 mm in diameter a spherical drop shape is desired but the ultra-sonic field causes an oblate deformation of the drop. This deformation is minimized by lowering the input power to the radiator or by increasing the distance between the radiator and the reflector plate which indirectly reduces the power of the ultra-sonic standing wave field. On the other hand, both adjustments lead to a reduced stability of the floated drop. Thus, these two factors, area of temperature observation and stability of the floated drop, require a compromise between a more stable flattened drop and a less stable spherical drop. Another disturbance is the tendency of the drops to oscillate, in particular directly after inserting the drop into the levitator. By temporarily increasing the distance between the radiator and the reflector plate, the initiated oscillations are restrained.

All measuring instruments were arranged around the acoustic levitator inside the cold chamber. Several windows in the protecting acrylic glass tube allow the observation of the levitated drops: a zinc selenide lens for the infra-red thermometer, an optical filter for the video camera, a hole for the Pt100 sensor, and, furthermore, a shutter to inject the drops. A Teflon-coated needle from which the drops could be easily released was used to place the drops at the ultrasonic standing wave node.

To control, record, and store the experimental parameters, a PC with the application software LabView was used. The images of the video camera were monitored on the outside PC so that the drop could be observed on-line during freezing and, afterwards, the drop sizes were determined. The transition from the liquid to the ice phase became visible from the change of the transparent liquid drop to an opaque frozen drop as recorded from the video camera. The exact definition of the onset of nucleation was obtained by the temporal evolution of the drop surface temperature recorded by the infra-red thermometer (see next section).

### 2.1.2 Experimental procedure

The investigated drops had sizes of 1 mm radius which is larger than cloud drops but is in the range of raindrops (Pruppacher and Klett, 1997). However, as mentioned above, this drop size was required to perform the measurement of the drop surface temperature. Before each set of experiments, the levitator was cleaned by rinsing with purified water and purity checks were performed to ensure that no particles were present in the environment of the floating drops to affect nucleation rather than by the particles immersed in the drops. Drops generated from

pure distilled and de-ionised water of 1 mm radius did not freeze within the experimental time periods of less than a minute at temperatures above -35°C which is to be expected when no ice nuclei are present (Pruppacher and Klett, 1997).

The measurement of the drop surface temperature allows to clearly determine the onset of freezing. Figure 2a shows an example for the temperature development during freezing. According to Hindmarsh et al. (2003) it can be divided into four stages: 1. Supercooling stage before the phase change sets in; here the temperature decreases. 2. Recalescence stage which is characterised by a sudden temperature increase. Latent heat is released when the phase change is initiated so that the surface temperature of the drop reaches almost 0°C. 3. Freezing stage which is a rather long time period where the entire drop freezes; at the end, the temperature decreases again; 4. Cooling stage after the drop is entirely frozen. Similar observations are reported by Bauerecker et al. (2008).

For the freezing experiments, the cold chamber was always pre-cooled to a low temperature around -30 ± 1°C. Thus, the cooling rate of the drops, i.e. the rate by which the drop temperature was adapted to the ambient temperature was the same during all experiments. The development of the drop surface temperature with time was measured several times with pure water drops. The drops reached a lowest temperature of -27 ± 0.7°C only because the levitator was isolated against the cold chamber air (see section 2.1.1). From the measurements the following equation was derived to describe the drop temperature $T_{drop}(t)$ in °C:

$$T_{drop}(t) = -27.050°C + 27.082°C \exp\left(-\frac{t}{16.374}\right) \quad (1)$$

with the time $t$ in s and the result is shown in Figure 2b. Drops were generated from distilled water which was mixed with the selected mineral dust particles in defined amounts. During the experiments, this solution was continuously stirred to avoid a settling and agglomeration of the particles. It was kept inside the cold chamber at a constant temperature slightly above 0°C. Individual drops were levitated one after another until they froze and the freezing temperatures, i.e. the lowest surface temperatures were recorded. For each particle type and concentration, approximately 100 drops were observed.

## 2.2 Vertical wind tunnel

In the Mainz vertical wind tunnel drops from micrometer to millimetre sizes are freely floated at their terminal velocities in a vertical air stream. Thus, ventilation and heat transfer are

similar to the situation as in the real atmosphere. The experiments were performed similar as described in Diehl et al. (2002) and v. Blohn et al. (2005) where immersion freezing of pollen was investigated. Detailed descriptions of the wind tunnel are given therein and in the review paper of Diehl et al. (2011). To perform ice nucleating experiments, the tunnel can be cooled down to -30°C. Ambient air sucked through the tunnel by means of two vacuum pumps. The air is passed through particle filters to avoid the presence of possible ice nuclei during the experiments. Before each series of experiments it was proven that pure water drops containing no particles did not freeze within the investigated temperature range. For the immersion freezing experiments, the wind tunnel was pre-cooled to certain temperatures in steps of 1K so that, in contrast to the acoustic trap experiments, drop freezing was observed at constant temperatures. Particles were mixed with distilled water in defined concentrations and drops formed from this mixture were injected into the wind tunnel. For each temperature and particle type, 40 to 50 drops were investigated. The onset of freezing was determined by observation and is characterized by an opaque look of the drops and a different floating behaviour.

As an improvement to earlier measurements (Diehl et al., 2002; v. Blohn et al., 2005), the fractions of frozen drops were determined time-resolved. When a drop started floating, a time recording was started until the drop froze. The total observation time per drop was 30 seconds, i.e. drops which did not freeze within this time period were counted as unfrozen. Wind speed, temperature, and relative humidity of the tunnel air were recorded continuously. These parameters were required to calculate the drop sizes and the drop surface temperatures.

To keep the drop floated in the observation section, the air velocity in the tunnel must equal the terminal velocity of the drop, as such the drop size can be determined from the recorded wind speed (v. Blohn et al., 2005). In order to obtain similar sized drops for the experiments, only those drops were observed which were suspended in a rather narrow wind speed range of $2.70 \pm 0.25$ m/s. From this terminal velocity the average drop size was calculated according to Pruppacher and Klett (1997) to $340 \pm 30$ µm. The drops observed in the wind tunnel were smaller than the ones used in the acoustic trap but still larger than cloud droplets. This was a required compromise as drop freezing was determined by visual observation. According to Pruppacher and Klett (1997, Chapt. 13) the actual drop temperature while suspended in the wind tunnel and the adaptation time, i.e. the time until the drop temperature is equal to the ambient temperature were calculated from the ambient tunnel air temperature and the dew

point of the tunnel air. As shown in Figure 2c, it takes between 3 and 5 seconds until the temperature of a 370 µm drop reaches the ambient temperature. For the present experimental conditions, an adaptation time of 5 seconds was assumed. The measurement accuracy of the drop temperature was estimated as ± 1K.

## 2.3 Particle samples

Several particle samples were used in the experiments. As first test ice nuclei in the acoustic levitator, montmorillonite K10 particles were selected which are commercially available and characterised by a specific surface area of 245 ± 20 $m^2 g^{-1}$ (Sigma Aldrich). The majority of the experiments were performed with illite particles. Two types of illite were used: illite IMt1 and illite NX. Illite IMt1 is available from the Clay Mineral Society and according to the manufacturer is consists of 85 to 90% illite and 10 to 15% quartz. Particle diameters range from less than 0.2 µm to larger than 63 µm with a maximum of the number size distribution at 1.2 µm (Köster, 1996). The BET specific surface area was determined to be 31.7 $m^2 g^{-1}$ (Hiranuma and Möhler, 2013). Illite NX was selected as a test aerosol to be used in the research group INUIT and has been investigated by several different techniques (Hiranuma et al., 2014). According to Broadley et al. (2012) illite NX might be used as a proxy for atmospheric dust as its composition is rather close to atmospheric mineral dust. Samples of the same order obtained from B+M Nottenkämper were distributed within the INUIT research group and the properties of the dust particles as well as their elemental composition were characterized. According to Hiranuma et al. (2014) the distributed sample is composed by 69% illite, 14% feldspar, 10% kaolinite, 3% calcite, and 3% quartz which is rather similar to the composition of the illite NX sample used by Broadley et al. (2012) (60.5% illite, 13.8% illite-smectite mixed layer, 9.8% feldspar, 7.2% kaolinite, 6.6% quartz, and 2.1% carbonate). Its number size spectrum shows a maximum at 0.3 µm diameter, particle sizes are varying from 0.03 to 10 µm and the BET specific surface area is 124.4 ± 1.5 $m^2 g^{-1}$ (Hiranuma et al, 2014). Within an error of 17% this value agrees with the findings of Broadley et al. (2012) (104.2 ± 0.7 $m^2 g^{-1}$).

The particles immersed in the drops were evaluated in terms of particle surface area per drop. From the particle concentrations in the stock solutions and the average drop sizes the particle masses per drop were calculated and afterwards, by using the BET specific particle surfaces, the particle surface areas per drop were determined. With illite IMt1 and illite NX particles, three different particle concentrations were investigated, with montmorillonite K10 only one

particle concentration. Two illite NX particle concentrations were investigated at the vertical wind tunnel also. The bulk solutions were selected in the way that in spite of the different drop sizes in the levitator and the wind tunnel the particle masses and surface areas per drop were similar. The cases are listed in Table 1.

## 3 Results and discussion

### 3.1 Frozen fractions and median freezing temperatures

#### 3.1.1 Results from acoustic levitator experiments

In general, the results indicate that immersion freezing is dependant on the particle surface area in the drop. This confirms the findings of other recent studies as, e.g., Murray et al. (2011), Broadley et al. (2012), and Hartmann et al. (2013). In the following Figure 3, same colours represent data for similar particle surface areas per drop. The fractions of frozen drops are accumulated data, i.e. the values at a certain temperature include the drops frozen at higher temperatures. Figures 3a and 3b show the fractions of frozen drops as a function of temperature for illite IMt1 and illite NX, respectively, as measured in the acoustic levitator. With decreasing particle surface areas in the drops the median freezing temperature decreases, too, but the differences are reduced towards lower particle surface areas, see Table 1. In case of illite IMt1, the median freezing temperature decreased from -18.8°C to -23.6°C when the particle surface area per drop was reduced by one order of magnitude from $7.0 \times 10^{-5}$ $m^2$ $drop^{-1}$ to $3.5 \times 10^{-6}$ $m^2$ $drop^{-1}$; in case of illite NX, $T_{50}$ decreased from -19.7°C to -23.7°C by reducing the particle surface area per drop by two orders of magnitude from $7.1 \times 10^{-5}$ $m^2$ $drop^{-1}$ to $7.1 \times 10^{-7}$ $m^2$ $drop^{-1}$. Differences between the two illite types with comparable particle surface areas are not significant as they are only slightly higher than the measurement accuracies (± 0.7K).

Figure 3c demonstrates the freezing behaviour of montmorillonite K10 in comparison to illite. Although it was present in the drops with a particle surface area of $2.5 \times 10^{-4}$ $m^2$ $drop^{-1}$, i.e. one order of magnitude higher than in the highest cases of illite IMt1 and NX ($7.0 \times 10^{-5}$ and $7.1 \times 10^{-5}$ $m^2$ $drop^{-1}$, respectively), its median freezing temperature, -20.6°C does not exceed the ones of illite IMt1 and NX (-18.8°C and -19.7°C).

### 3.1.2 Results from wind tunnel experiments

Figure 4 gives the fractions of frozen drops as function of temperature for illite NX as measured in the wind tunnel for comparable particle surface areas in the drops (represented by same colours as before in Figure 3b). The figure shows accumulated data for the total observation time of 30 seconds. The median freezing temperatures (i.e. where half of the drops freeze within the 30 s observation time) were -20.8 ± 1°C and -19.2 ±1°C for particle surface areas of 5.1 × $10^{-6}$ $m^2$ $drop^{-1}$ and 5.1 × $10^{-5}$ $m^2$ $drop^{-1}$, respectively. Thus, the deviations between the results from the two techniques are within the measurement uncertainties (see Table 1). This agreement indicates that ventilation and heat transfer as present around a supercooled drop freely floated in the wind tunnel air stream is not significantly affecting ice nucleation.

## 3.2 Application of heterogeneous freezing models

### 3.2.1 Stochastic model

The stochastic model is based on classical nucleation theory and is used in a phenomenon way to interpret observations (see, e.g., Niedermeier et al. (2010) for more details about classical nucleation theory; Rigg et al., 2013). As it represents a physical description it can be applied even outside the range of surface areas and time scales investigated in the laboratory. It is initiated by the description of homogeneous freezing where it is assumed that small clusters randomly form in the supercooled liquid phase, only some of them growing further to macroscopic crystals (e.g., Pruppacher and Klett, 1997; Murray et al., 2010). In case that a solid surface is present this stabilizes the clusters of the ice phase. To extend the homogeneous stochastic model to heterogeneous ice nucleation by a single species it is assumed that the nucleating probability is equal for all drops of a population. Thus, the number of drops $\Delta n_{fr}$ freezing heterogeneously in a time period $\Delta t$ is given by (Murray et al., 2011):

$$\Delta n_{fr} = N_{total}(1 - \exp(-J(T)\, s\, \Delta t)) \qquad (2)$$

with $N_{total}$ the total number of observed drops, $s$ the particle surface area immersed in the drops, and $J(T)$ the nucleation rate coefficient per unit particle surface area and time. With $f_{ice}$ meaning the fraction of frozen drops

$$f_{ice} = \frac{n_{fr}}{N_{total}} \qquad (3)$$

as determined in the experiments, and the freezing time *t,* the nucleation rate coefficients *J(T)* per unit particle surface area and time can be calculated according to Murray et al. (2011):

$$J(T) = -\frac{\ln\left(1 - f_{ice}\right)}{s\,t} \qquad (4)$$

As Equation 4 is valid for constant temperatures it is applicable to the wind tunnel experiments only. Following Koop et al. (1997) the freezing time *t* can be interpreted as the total cumulative observation time, i.e. 30 seconds as due to the stochastic model each freezing event is independent on the number of previous trials and the different freezing events are not dependant on each other. Figure 5 shows the nucleation rate coefficients *J(T)* for illite NX present with 5.1 $\times 10^{-6}$ m$^2$ per drop and 5.1 $\times 10^{-5}$ m$^2$ per drop derived from the wind tunnel experiments by using Equation 4. For the limited ranges of particle surface area and temperature the nucleation rate coefficients can be described by a single line within the experimental errors (black line in Figure 5) thus indicating that the log of the nucleation rate coefficient increases with temperature.

The time-resolved measurements of the frozen fractions at constant temperatures at the wind tunnel were used to look closer to the time dependence of freezing. The liquid ratio, i.e. the fractions of drops which remain liquid were calculated as function of time. From Equation 2 it can be derived that

$$\ln\frac{n_{liq}}{N_{total}} = -J(T)\,s\,t \qquad (5)$$

and the results are given in Figure 6 for 5.1 $\times 10^{-6}$ m$^2$ per drop and 5.1 $\times 10^{-5}$ m$^2$ per drop, respectively, for different temperatures. The adaption time is marked in Figure 6 as vertical dashed-dotted lines. At a given temperature, e.g., -21°C freezing proceeds more slowly with the lower particle surface area 5.1 $\times 10^{-6}$ m$^2$ per drop (see blue symbols in Figure 6). So it is expected that at lower temperatures and with higher particle surface areas per drop freezing proceeds faster. Such behaviour has been observed also by Murray et al. (2011) and Broadley et al. (2012) in isothermal experiments. On the left-hand-side of the vertical line, the logarithm of the liquid ratio decreases non-linearly with time. In these cases freezing took place before the drops had reached the ambient temperature, i.e. they froze at higher temperatures. Regarding the cases on the right-hand-side of the vertical line, one can note that except for one case (at -21°C with s = 5.1 $\times 10^{-6}$ m$^2$ per drop) the data rather well follow

straight lines which were drawn starting at $t$ = 5 s (adaption time), see dotted lines in Figure 6. They indicate the exponential decay of the liquid drops with time at constant temperatures as predicted by Equation 5. This confirms that nucleation events during the wind tunnel experiments were time-dependant stochastic processes in agreement with classical nucleation theory.

To apply the stochastic model to the data measured with the acoustic trap one has to consider the effect of the non-linear cooling rate. For that purpose Equation 4 was modified as follows. It was assumed that during temperature changes of 1K the cooling rate was nearly constant. This value was selected as the data were evaluated in steps of 1K due to the temperature measurement error of 0.7K. For each temperature in steps of 1K the total cooling time $t$ was calculated according to Equation 1. Afterwards, for each temperature change $\Delta T$ the required time $\Delta t$ was calculated and the cooling rate $\gamma(T)$ was determined from

$$\gamma(T) = \frac{\Delta T}{\Delta t} \tag{6}$$

with $\Delta T$ = 1K. Thus, for a temperature change from $T_1$ to $T_2$ there is a cooling rate according to Equation 6 and the change of the frozen fraction is given by

$$\Delta\left(\frac{n_f}{N_{total}}\right) = \frac{\Delta n_f}{N_{total}} = \frac{n_{f,2}}{N_{total}} - \frac{n_{f,1}}{N_{total}} \tag{7}$$

considering that $N_{total}$ is constant. Analogous to Equation 2, the number of drops $\Delta n_{fr}$ freezing heterogeneously during a temperature change $\Delta T$ is given by

$$\Delta n_f = N_{total}\,(1 - \exp(-J(T)\; s\; \Delta T \frac{1}{\gamma(T)})) \tag{8}$$

with the cooling rate $\gamma$ in units of [K $s^{-1}$] and the nucleation rate coefficient $J(T)$ in units of [$area^{-1} \cdot s^{-1}$]. Thus, $J(T)$ can be calculated by

$$J(T) = -\frac{\ln\left(1 - \Delta\frac{n_n}{N_{total}}\right)}{s\,\Delta T\,\frac{1}{\gamma(T)}} \tag{9}$$

with $\Delta T$ = 1K.

A comparison of the nucleation rate coefficients derived from acoustic levitator and wind tunnel measurements is given in Figure 7. Results from wind tunnel experiments (derived according to Equation 4) are shown with their regression line (solid line in black) as in Figure

5. The dotted black line gives the extrapolation of the regression line towards higher and lower temperatures. Results from acoustic trap experiments were calculated by using the modified Equation 9. They show a rather large scatter around the regression line; however, in the temperature range below -17°C they follow the same trend. At higher temperatures the data are located definitely above the extrapolated regression line. This indicates that in the acoustic levitator experiments the freezing rate of the drops during the first 15 seconds of cooling is overestimated because of the very fast cooling rate in the beginning.

### 3.2.2 Singular model

Besides the stochastic model, it is suggested that heterogeneous freezing is dominated by the nucleating characteristics of ice-active sites and, thus, only dependant on temperature while the time-dependence, i.e. the stochastic nature of the freezing process becomes negligible (Vali, 2008). The singular model is based on the assumption that critical clusters form on ice-active sites at characteristic temperatures so that freezing takes place as soon as the characteristic temperature is reached without any time dependence. Therefore, if the temperature is held constant one would not observe further freezing events. However, this is not consistent with the present wind tunnel observations and previous measurements (e.g., Murray et al., 2011; Broadley et al., 2012). Thus, the singular model is not a physical description as the stochastic model and, therefore, its application is restricted to the experimental conditions under which the data were obtained. In spite of this the singular model is used here to compare the data obtained by the two different techniques where in one case the drops were kept at constant temperatures, in the other they cooled down with a non-linear cooling rate.

Under the assumption that the ice nuclei immersed in the drops show just one type of nucleation site, the singular model predicts that every drop will freeze at the same time as soon as the characteristic temperature is reached under cooling. In an experiment where the drops contain different types of ice nuclei one would observe a distribution of characteristic temperatures. The fraction of drops $f_{ice}$ freezing at a temperature $T$ is given by (Connolly et al., 2009; Niedermeier et al., 2010):

$$f_{ice} = \frac{n_{fr}}{N_{total}} = 1 - \exp\left(-n_s(T)\, s\right) \qquad (10)$$

with $n_{fr}$ the number of frozen drops, $N_{total}$ the total number of observed drops, $s$ the particle surface area immersed in the drops, and $n_s(T)$ the number of active sites per surface area $s$ which are active within the temperature range from 0°C to $T$. The differential nucleus spectrum $k(T)$ and the number density of active sites $n_s(T)$ are related as follows when lowering the temperature from $T_0 = 0$°C to $T$ (Broadley et al., 2012):

$$n_s(T) = -\int_{T_0}^{T} k(T)\, dT \qquad (11)$$

From the present data the surface density of active sites $n_s(T)$ per unit particle surface area was determined by (Murray et al., 2011):

$$n_s(T) = -\frac{\ln\left(1 - f_{ice}\right)}{s} \qquad (12)$$

Figure 8a shows the surface densities of active sites $n_s$ for illite NX from both techniques, marked by different colours, for all investigated particle surface areas per drop. The two data sets show a very good agreement within the measurement errors and are represented by one third order polynomial regression curve (solid black line). The data measured with illite IMt1 (Figure 8b) follow a somewhat different trend so that they are represented by another third order polynomial regression curve. A comparison of these regression curves as shown in Figure 8c (blue and black symbols and lines) indicates that they cross each other at a temperature of -19°C. The deviations in the other temperature ranges are in most cases slightly outside the measurement errors. In contrast, the results from montmorillonite K10, additionally shown in Figure 8c in red, lie below the curves for illite and follow another trend. Although data are available only for a limited temperature range this trend indicates a reduced surface density of active sites of montmorillonite which is to be expected according to the results of Atkinson et al. (2013). In general, Figure 8 indicates that the lower the temperature the more active sites are available on the ice nucleating material.

### 3.2.3 Comparison to literature data

The immersion freezing behaviour of illite NX was investigated by Broadley et al. (2012) for particle surface areas between $1 \times 10^{-11}$ m$^2$ to $3 \times 10^{-8}$ m$^2$ corresponding to drops with radii between 5 and 40 µm. Thus, in their experiments the drop volumes were at least 4 orders of magnitudes smaller and so were the particle surface areas. The nucleation rate coefficients and surface densities of active sites from the present experiments are compared to the results

of Broadley et al. (2012) for immersion freezing of illite NX. In Figure 9, the area of the Broadley et al. (2012) nucleation rate coefficients for various cooling rates and different particle surface areas between $1 \times 10^{-11}$ m$^2$ to $3 \times 10^{-8}$ m$^2$ is marked as a grey shaded area. The present results are shown as blue and red symbols (results from acoustic levitator and wind tunnel, respectively). Because of higher particle surface areas they are located in a completely different temperature range but the trend towards lower temperatures shows that they approximate the Broadley et al. (2012) results. In Figure 10 the surface densities of active sites for illite NX from the present experiments (shown as blue and red symbols, polynomial regression curve from the data as solid line) are compared to the results from Broadley et al. (2012) (green solid line as fit to the data, from Broadley et al., 2012). Although there is a gap between the two lines at a temperature of -25°C both datasets follow a similar exponential trend. These comparisons indicate that the present results very well complement the results from Broadley et al. (2012) as the trends observed for lower particle surface areas are confirmed by the present results in the higher temperature range.

## 4 Summary and conclusions

Immersion freezing was found to occur in a temperature range between -14 and -26°C in dependence of particle type and surface area per drop. The rather high freezing temperatures are due to the drop sizes of 340 μm and 1 mm in radius and, thus, large particle masses and surface areas per drop. The data were evaluated in terms of nucleation rate coefficients and surface densities of active sites according to both the stochastic and singular models of heterogeneous freezing. The observations in the wind tunnel indicate that ice nucleation affected by mineral dust particles proceeds with time and, thus, the stochastic description is supported by the present findings and verifies that ice nucleation affected by illite and montmorillonite follows the classical nucleation theory. Nucleation rate coefficients were determined from wind tunnel with the use of the total observation time as freezing time. For the measurements in the acoustic trap, a modification was required to account for the non-linear cooling rate of the drops. This was undertaken by using piecewise linear cooling rates. The resulted nucleation rate coefficients agree well with the ones derived from wind tunnel experiments for temperatures lower than -17°C.

Although the singular model which neglects time dependence of nucleation does not account for the observations that freezing proceeds with time at constant temperatures, its application

to the present wind tunnel and acoustic trap results shows a good agreement between the two experimental techniques for the surface densities of active sites.

The present results for illite NX and illite IMt1 are in agreement with previous studies of Broadley et al., 2012 and extend the temperature range of the nucleation rate coefficients and the surface site densities towards higher temperatures. The results of the two types of illite are similar although their composition is somewhat different. The findings for montmorillonite K10 indicate a trend towards a lower surface density of ice-active sites as suggested by Atkinson et al. (2013).

The two techniques used in the present investigations both allow to freely suspend single drops without any wall or substrate contacts but having the disadvantage that the drop sizes are larger than typical cloud drops. In the wind tunnel, the drops reach equilibrium with the ambient temperature within 3 to 5 seconds and, afterwards, remain at a constant temperature during observation. This allows to observe any time dependence of the freezing process. In the acoustic levitator, it is not possible to cool down the drops within seconds because of the larger drop volume and the missing ventilated heat transfer. Therefore, they cool down more slowly exchanging heat with the ambient air in the cold chamber which, because of the large drop volume, results in a non-linear cooling rate.

In spite of some deficiencies the use of the acoustic levitator has a number of essential advantages. It is a small transportable instrument and can be easily installed. It does not require a large air flow and, thus, energy to establish drop floating and is, therefore, much more economical in its operation. Although in the present experiments the levitator was placed inside a walk-in cold chamber, it might as well be placed inside a table top cold box. The possibility to directly measure the drop temperature with an infra-red thermometer allows to clearly define the onset of freezing. In particular for nucleation processes, flow hydrodynamics and ventilated heat transfer as it happens in the wind tunnel are not deciding factors as much as the temperature and the cooling rate. This is validated by the good agreement of the results from the two techniques. If required, a small design modification could bring additional ventilated heat transfer. Thus, the acoustic levitator presents a good alternative to other methods to investigate drop freezing in the immersion mode.

The present results contribute to a data base on which parameterizations applicable in cloud models are derived. The special mineral dust type illite NX has been investigated by a number of different experimental techniques within the frame work of INUIT. A compilation of all

results from the entire INUIT community with a general parameterization applicable to model simulations is presented in the joint publication of Hiranuma et al. (2014).

## Acknowledgements

This work is part of the research group INUIT (Ice Nuclei research UnIT) and was supported by the Deutsche Forschungsgemeinschaft under grant DI 1539/1-1. We would like to acknowledge the expertise of T. Kisely (Karlsruhe Institute of Technology, Institute for Nuclear Waste Disposal) for the BET measurements of the used illite particle samples.

## References

Bauerecker, S., Ulbig, P., Buch, V., Vrbka, L., and Jungwirth, P.: Monitoring ice nucleation in pure and salty water via high-speed imaging and computer simulations. J. Phys. Chem. C, 112, 7631-7636, 2008.

v. Blohn, N., Mitra, S.K., Diehl, K., and Borrmann, S: The ice nucleating ability of pollen. Part III: New laboratory studies in immersion and contact freezing modes including more pollen types. Atm. Res., 78, 182-189, 2005.

Broadley, S.L., Murray, B.J., Herbert, R.J., Atkinson, J.D., Dobbie, S., Malkin, T.L., Condliffe, E., and Neve, L., 2012: Immersion mode heterogeneous ice nucleation by an illite rich powder representative of atmospheric mineral dust. Atmos. Chem., Phys., 12, 287-307, doi:10.5194/acp-12-287-2012.

Connolly, P. J., Möhler, O., Field, P. R., Saathoff, H., Burgess, R., Choularton, T., and Gallagher, M.: Studies of heterogeneous freezing by three different desert dust samples, Atmos. Chem. Phys., 9, 2805–2824, doi:10.5194/acp-9-2805-2009, 2009.

DeMott, P. J., Chen, Y., Kreidenweis, S. M., Rogers, D. C., and Sherman, D. E.: Ice formation by black carbon particles, Geophys. Res. Lett., 26, 2429–2432, 1999.

Diehl, K., Matthias-Maser, S., Mitra, S.K., and Jaenicke, R.: The ice nucleating ability of pollen. Part II: Laboratory studies in immersion and contact freezing modes, Atmos. Res., 61, 125-133, 2002.

Diehl, K., Simmel, M., and Wurzler, S.: Numerical simulations of the impact of aerosol properties and drop freezing modes on the glaciation, microphysics, and dynamics of clouds, J. Geophys. Res., 111, D07202, doi:10.1029/2005JD005884, 2006.

Diehl, K., Ettner-Mahl, M., Hannemann, A., and Mitra, S.K.: Homogeneous freezing of single sulfuric and nitric acid solution drops levitated in an acoustic trap, Atm. Res., 94, 356-361, doi:10.1016/j.atmosres.2009.06.001, 2009.

Diehl, K., Mitra, S.K., Szakáll, M., v. Blohn, N., Borrmann, S., and Pruppacher, H.R.: The Mainz vertical wind tunnel facility: A review of 25 years of laboratory experiments on cloud physics and chemistry, in: J.D. Pereira (Ed.), Wind tunnels: Aerodynamics, models, and experiments. Nova Science Publishers, Inc., Chapter 2, 2011.

Duft, D., and Leisner, T: Laboratory evidence for volume-dominated nucleation of ice in supercooled water microdroplets, *Atmos. Chem. Phys.,* **4,** 1997-2000, 2004.

Ettner, M., Mitra, S.K., and Borrmann, S.: Heterogeneous freezing of single sulphuric acid solution droplets: laboratory experiments utilizing an acoustic levitator, Atmos. Chem. Phys., 4, 1925-1932, 2004.

Hartmann, S., Augustin, S., Clauss, T., Voigtländer, J., Niedermeier, D., Wex, H., and Stratmann, F.: Immersion freezing of ice nucleating active protein complexes, Atmos. Chem. Phys., 13, 5751-5766, doi:10.5194/acp-13-5751-2013, 2013.

Hindmarsh, J. P., Russell, A.B. and Chen, X.D.: Experimental and numerical analysis of the temperature Transition of a suspended freezing water droplet, Intern. J. Heat and Mass Transfer, 46, 1199-1213, 2003.

Hiranuma, N, and Möhler, O.: Pers. comm., 2013.

Hiranuma, N., et al. (44 co-authors): A comprehensive laboratory study on the immersion freezing behavior of NX-illite particles: a comparison of seventeen ice nucleation measurement techniques, Atmos. Chem. Phys. Discuss., 14, 22045-22116, doi:10.5194/acpd-14-22045-2014, 2014.

Hoffer, T.E.: A laboratory investigation of droplet freezing, J. Meteor., 18, 766-778, 1961.

Hoose, C., Lohmann, U., Erdin, R., and Tegen, I.: The global influence of dust mineralogical composition on heterogeneous ice nucleation in mixed-phase clouds, Environ. Res. Lett., 3, 025003-025017, 2008.

Hoose, C., and Möhler, O.: Heterogeneous ice nucleation on atmospheric aerosols: a review of results from laboratory experiments, Atmos. Chem. Phys., 12, 9817-9854, doi:10.5194/acp-12-9817-2012, 2012.

INUIT Research group website: www.ice-nuclei.de.

Kandler, K., Benker, N., Bundke, U., Cuevas, E., Ebert, M., Knippertz, P., Rodríguez, S., Schütz, L., and Weinbruch, S.: Chemical composition and complex refractive index of Saharan mineral dust at Izaña, Tenerife (Spain), derived by electron microscopy, Atmos. Environ., 41, 8058–8074, doi:10.1016/j.atmosenv.2007.06.047, 2007.

Kanji, Z.A., DeMott, P.J., Möhler, O., and Abbatt, J.P.D.: Results from the University of Toronto continuous flow diffusion chamber at ICIS 2007: instrument intercomparison and ice onsets for different aerosol types, Atmos. Chem. Phys., 11, 31-41, doi:10.5194/acp-11-31-2001, 2011.

Köster, H. M.: Mineralogical and chemical heterogeneity of three standard clay mineral samples, Clay Minerals, 31, 417-422, 1996.

Koop, T., Luo, B.P., Biermann, U.M., Crutzen, P.J., and Peter, T.: Freezing of $HNO_3/H_2SO_4/H_2O$ solutions at stratospheric temperatures: Nucleation statistics and experiments, J. Phys. Chem. A, 101, 117-1133, 1997.

Koop, T., L. Beiping, A. Tsias, and T. Peter, 2000: Water activity as the determinant for homogeneous ice nucleation in aqueous solutions. Nature, 406, 611-614.

Ladino, L., Stetzer, O., and Lohmann, U.: Contact freezing: a review. Atmos. Chem. Phys. Discuss., 7811-7869, 2013.

Leng, Y., and Cummings, P.T.: Hydration structure of water confined between mica surfaces, J. Chem. Phys., 124**,** 074711, 2006.

Lüönd, F., Stetzer, O., Welti, A., and Lohmann, U.: Experimental study on the ice nucleation ability of size selected kaolinite particles in the immersion mode, J. Geophys. Res., 115, D14201, doi:10.1029/2009JD012959, 2010.

Marcolli, C., Gedamke, S., Peter, T., and Zobrist, B., Efficiency of immersion mode ice nucleation on surrogates of mineral dust, Atmos. Chem. Phys., 7, 5081-5091, doi:10.5194/acp-7-5081-2007. 2007.

Möhler, O., Stetzer, O., Schäfers, S., Linke, C., Schnaiter, M., Tiede, R., Saathoff, H., Krämer, M., Mangold, A., Budz, P., Zink, P., Schreiner, J., Mauersberger, K., Haag, W., Kärcher, B., and Schurath, U.: Experimental investigation of homogeneous freezing of

sulphuric acid particles in the aerosol chamber AIDA, Atmos. Chem. Phys., 3, 211–223, 2003.

Murray, B.J., Broadly, S.L., Wilson, T.W., Bull, S., and Wills, R.H.: Kinetics of the homogeneous freezing of water, Phys. Chem. Chem. Phys., 12, 10380-10387, doi:10310.11039/c003297b, 2010.

Murray, B.J., Wilson, T.W., Broadly, S.L., and Wills, R.H.: Heterogeneous freezing of water droplets containing kaolinite and montmorillonite particles, Atmos. Chem. Phys., 11, 4191-4207, doi:10.5194/acp-11-4191-2011, 2011.

Niedermeier, D., Hartmann, S., Shaw, R. A., Covert, D., Mentel, T. F., Schneider, J., Poulain, L., Reitz, P., Spindler, C., Clauss, T., Kiselev, A., Hallbauer, E., Wex, H., Mildenberger, K., and Stratmann, F.: Heterogeneous freezing of droplets with immersed mineral dust particles – measurements and parameterization, Atmos. Chem. Phys., 10, 3601–3614, doi:10.5194/acp-10-3601-2010, 2010.

Niemand, M., Möhler, O., Vogel, B., Vogel, H., Hoose, C., Connolly, P., Klein, H., Bingemer, H., Skrotzki, J., and Leisner, T.: A particle-surface-area-based parameterization of immersion freezing on mineral dust particles, J. Atmos. Sci., 69, 3077-3092, doi:10.1175/JAS-D-11-0249.1, 2012.

Phillips, V.T.J., Donner, L.J., and Garner, S.T.: Nucleation processes in deep convection simulated by a cloud-system-resolving model with double-moment bulk microphysics, J. Atmos. Sci., 64, 738-761, 2007.

Pinti, V., Marcolli, C., Zobrist, B., Hoyle, C.R., and Peter, T.: Ice nucleation efficiency of clay minerals in the immersion mode, Atmos. Chem. Phys., 12, 5859-5878, 2012.

Pitter, R.L., and Pruppacher, H.R.: A wind tunnel investigation of freezing of small water drops falling at terminal velocity in air, Quart. J. Roy. Meteor. Soc., 99, 540-550, 1973.

Pruppacher, H.R., Klett, J.D.: Microphysics of Clouds and Precipitation, 2nd rev. ed., Kluwer Academic Publishers, Dordrecht, 1997.

Pummer, B. G., Bauer, H., Bernardi, J., Bleicher, S., and Grothe, H.: Suspendable macromolecules are responsible for ice nucleation activity of birch and conifer pollen, Atmos. Chem. Phys., 12, 2541–2550, doi:10.5194/acp-12-2541-2012, 2012.

Rigg, Y.J., Alpert, P.A., and Knopf, D.A.: Immersion freezing of water and aqueous ammonium sulphate droplets initiated by humic-like substances as a function of water activity. Atmos. Chem. Phys., 13, 6603-6622, doi:10.5194/acp-13-6603-2013, 2013.

Storelvmo, T., Kristjánsson, J. E., and Lohmann, U.: Aerosol influence on mixed-phase clouds in CAM-Oslo, J. Atmos. Sci., 65, 3214–3230, 2008.

Vali, G.: Repeatability and randomness in heterogeneous freezing nucleation, Atmos. Chem. Phys., 8, 5017-5031, 2008.

Zuberi, B., Bertram, A. K., Cassa, C. A., Molina, L. T., and Molina, M. J.: Heterogeneous nucleation of ice in (NH4)2SO4−H2O particles with mineral dust immersions, Geophys. Res. Lett., 29, 1504, doi:10.1029/2001GL014289, 2002.

Table 1. Experimental conditions during freezing experiments.

| particle type | specific surface area $m^2\ g^{-1}$ | drop radius mm | particle surface area $m^2\ drop^{-1}$ | median freezing temperature °C |
|---|---|---|---|---|
| montm. K10 | 245 | 1 ± 0.1 | $(2.5 \pm 0.3) \times 10^{-4}$ | -20.6 ± 0.7 |
| illite IMt1 | 31.7 | 1 ± 0.1 | $(3.5 \pm 0.4) \times 10^{-6}$ | -23.6 ± 0.7 |
| | | 1 ± 0.1 | $(3.5 \pm 0.4) \times 10^{-5}$ | -22.1 ± 0.7 |
| | | 1 ± 0.1 | $(7.0 \pm 0.7) \times 10^{-5}$ | -18.8 ± 0.7 |
| illite NX | 124.4 | 1 ± 0.1 | $(7.1 \pm 0.7) \times 10^{-7}$ | -23.7 ± 0.7 |
| | | 1 ± 0.1 | $(7.1 \pm 0.7) \times 10^{-6}$ | -22.8 ± 0.7 |
| | | 1 ± 0.1 | $(7.1 \pm 0.7) \times 10^{-5}$ | -19.7 ± 0.7 |
| | | 0.34 ± 0.03 | $(5.1 \pm 1.3) \times 10^{-6}$ | -20.8 ± 1.0 |
| | | 0.34 ± 0.03 | $(5.1 \pm 1.3) \times 10^{-5}$ | -19.2 ± 1.0 |

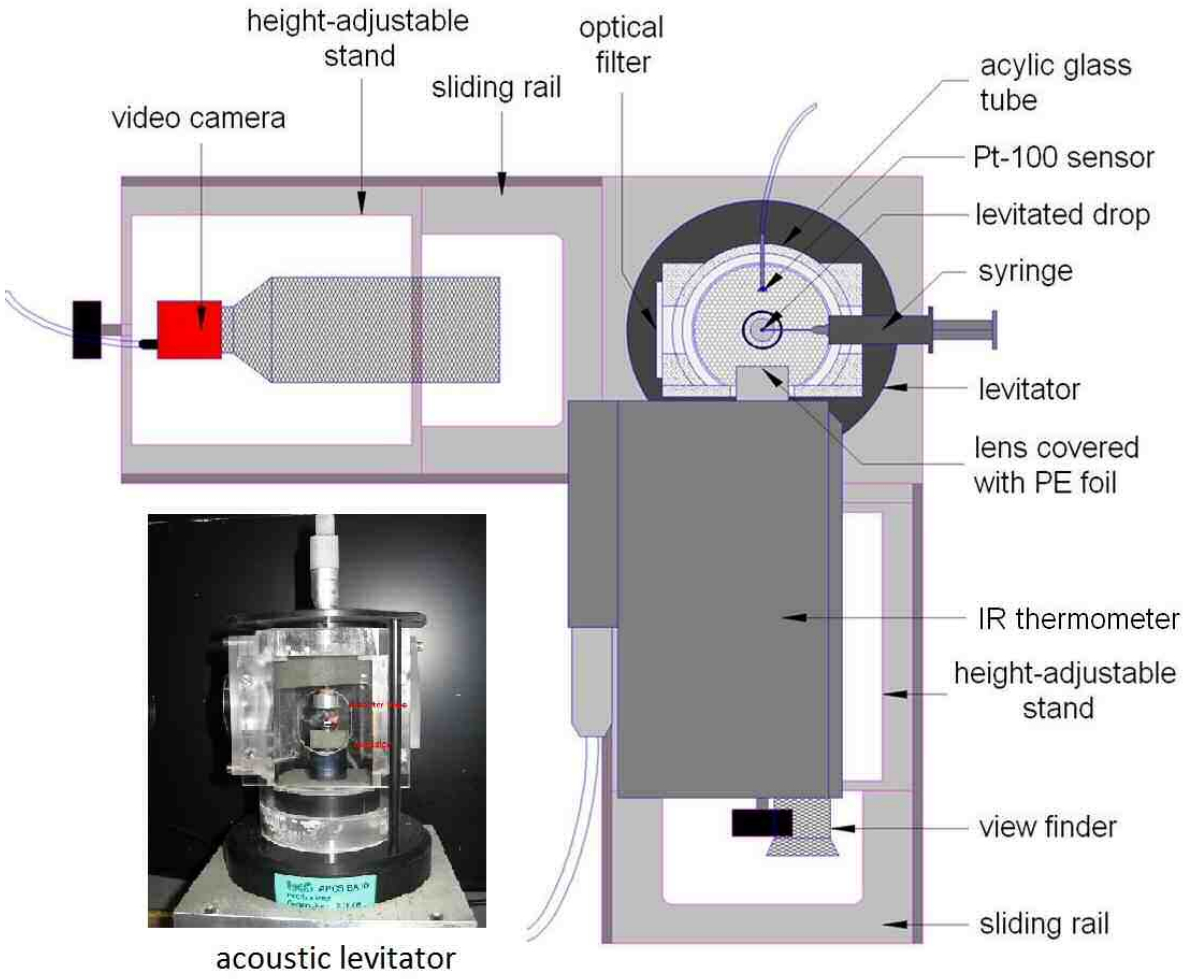


Figure 1: Scheme of the experimental setup in the cold chamber, view from above; left side: picture of the acoustic levitator.

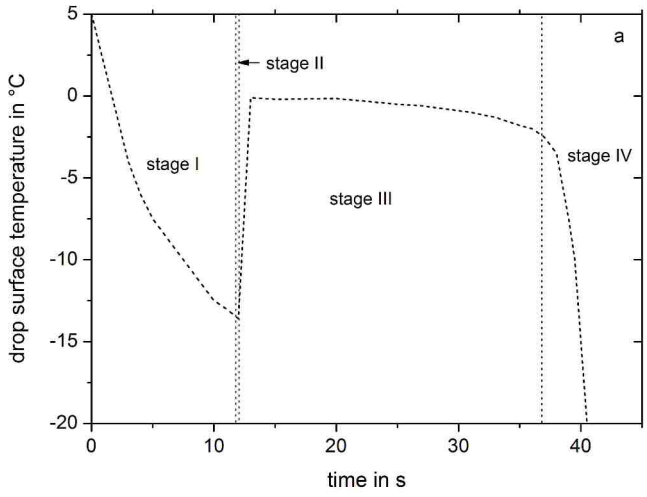


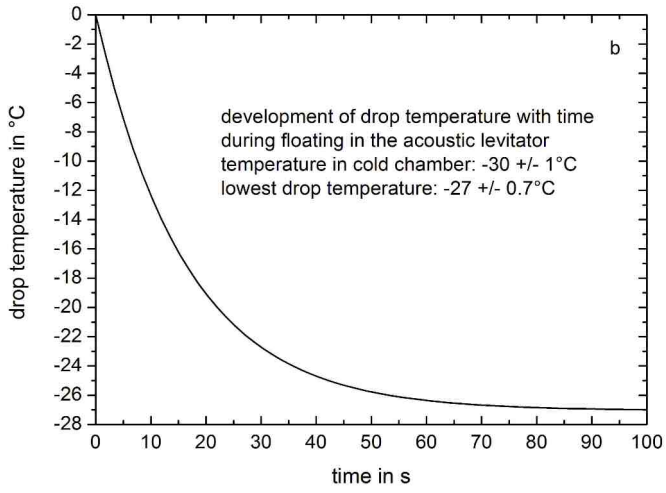


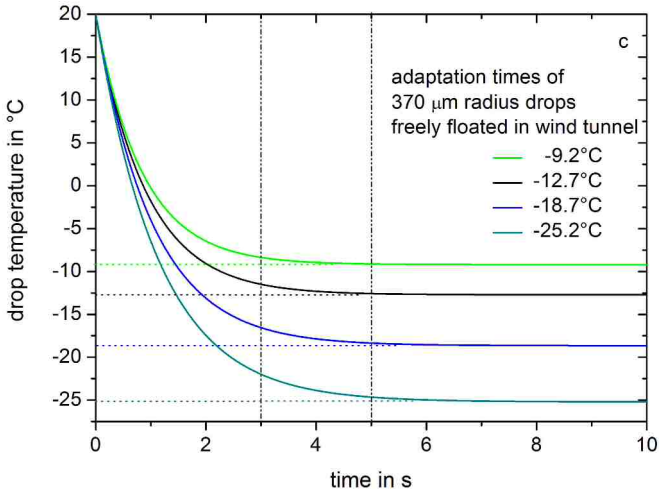


Figure 2: Experimental temperature trajectories. 2a: Example of the development of the drop temperature with time during freezing in the acoustic levitator. 2b: Development of drop temperature during freely floating in the acoustic levitator at a cold chamber ambient temperature of -30°C. 2c: Calculated adaptation times of 370 radius drops while freely floating in the wind tunnel at various ambient temperatures.

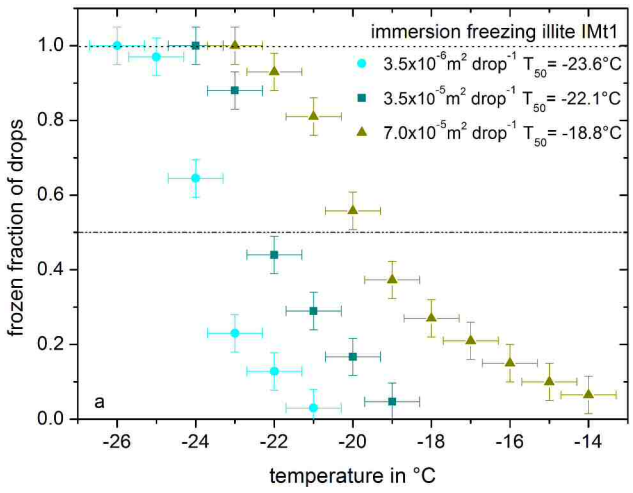


1

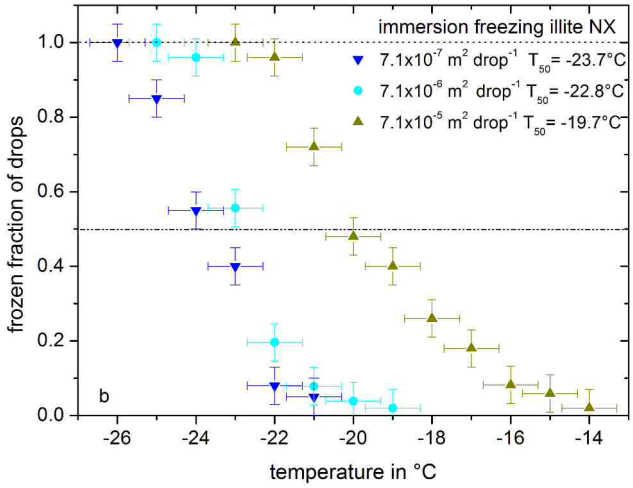


2

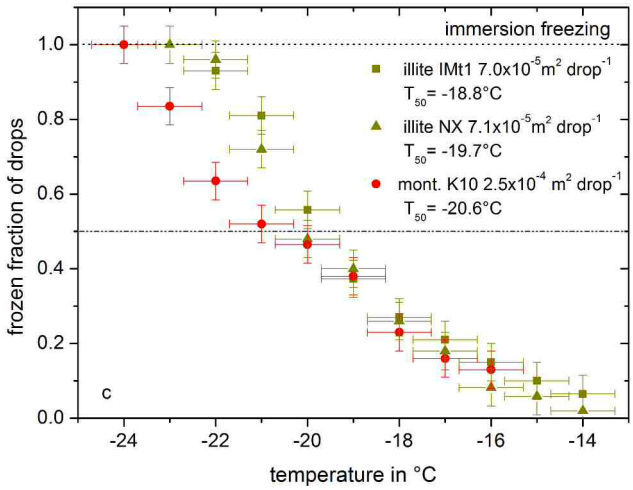


3

4 Figure 3: Immersion freezing in the acoustic levitator: frozen fractions of drops as function of
5 temperature for different particle surface areas per drop. 3a: Illite IMt1. 3b: Illite NX. 3c:
6 Montmorillonite K10 in comparison to illite.

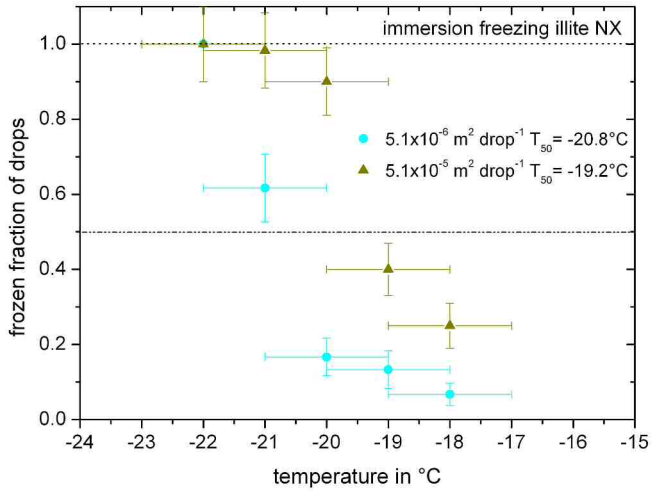


Figure 4: Immersion freezing of illite NX in the wind tunnel: frozen fraction of drops as function of temperature for two different particle surface areas per drop. Accumulated values within total observation time of 30 seconds.

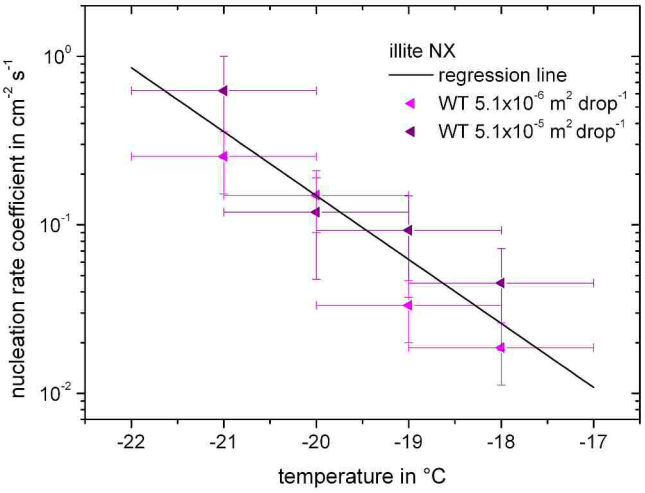


Figure 5: Nucleation rate coefficients as function of temperature for illite NX for two particle surface areas per drop, investigated in the wind tunnel.

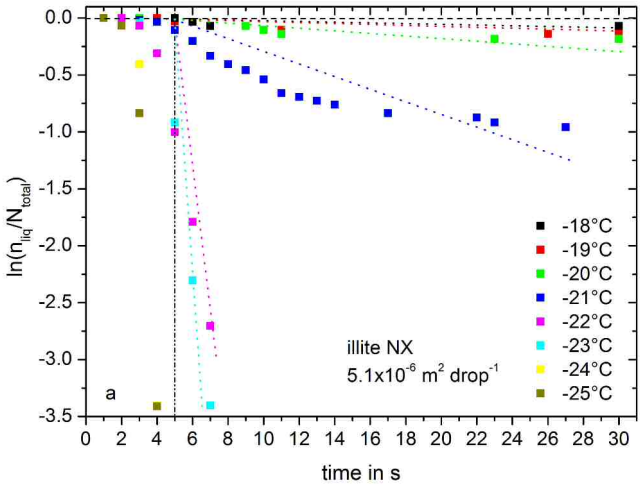


1

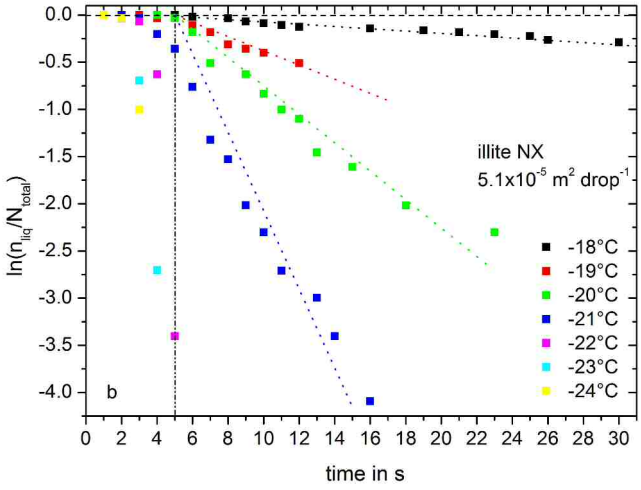


2

3 Figure 6: Liquid ratio as function of time from wind tunnel experiments with illite NX at
4 different temperatures. Vertical line: limit of adaptation time of the drops. 6a: Particle surface
5 area $5.1 \times 10^{-6}$ $m^2$ per drop. 6b: Particle surface area $5.1 \times 10^{-5}$ $m^2$ per drop. Dotted lines:
6 manually drawn starting at $t = 5$ s.

7

8

9

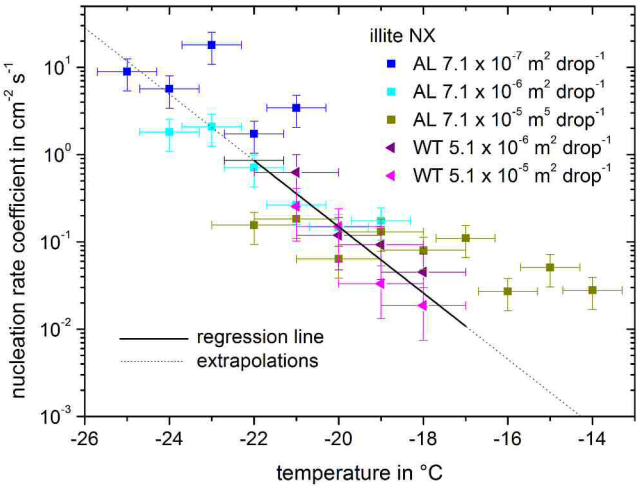


Figure 7: Nucleation rate coefficients as function of temperature for illite NX for various particle surface areas per drop, determined by two experimental techniques.

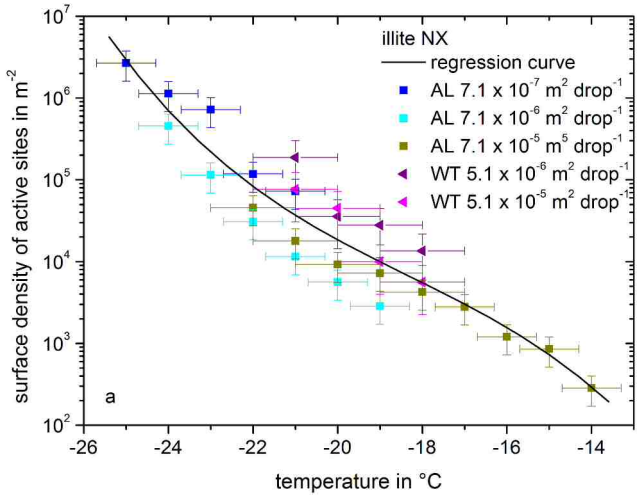


1

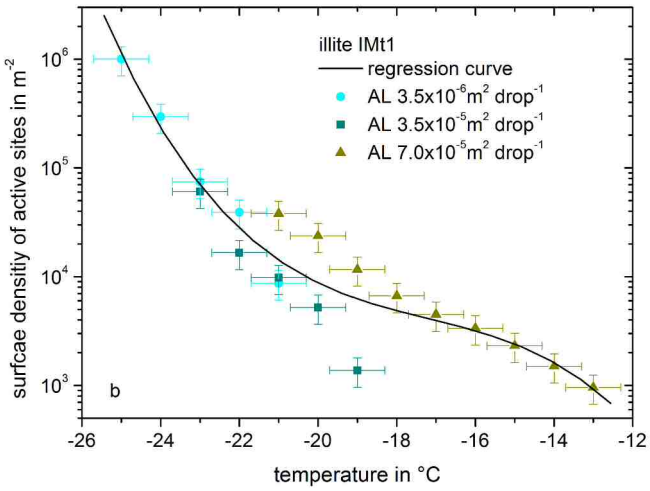


2

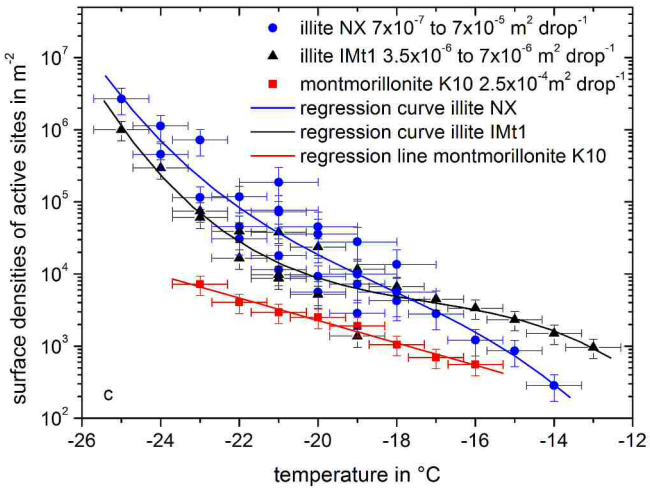


3

4 Figure 8: Surface densities of active sites as function of temperature for various particle
5 surface areas per drop. 8a: Illite NX, determined by the acoustic levitator (AL) and the wind
6 tunnel (WT). 8b: Illite IMt1, determined by the acoustic levitator. 8c: Comparison of
7 montmorillonite K10, illite NX, and illite IMt1.

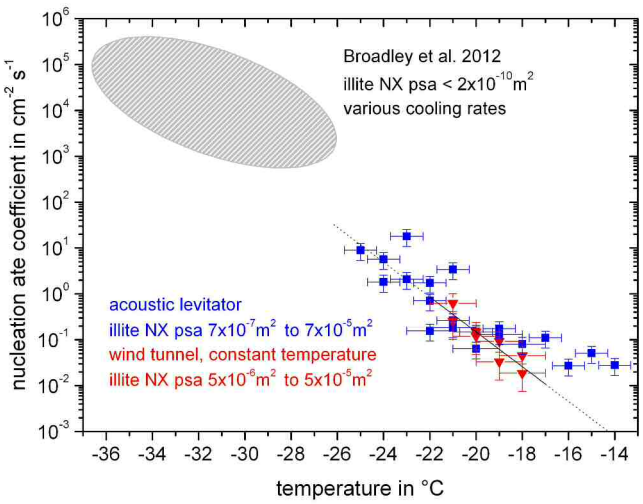


Figure 9: Nucleation rate coefficients as function of temperature for illite NX derived from present (shown in blue and red) and previous experiments (indicated as grey region, from Broadley et al., 2012).

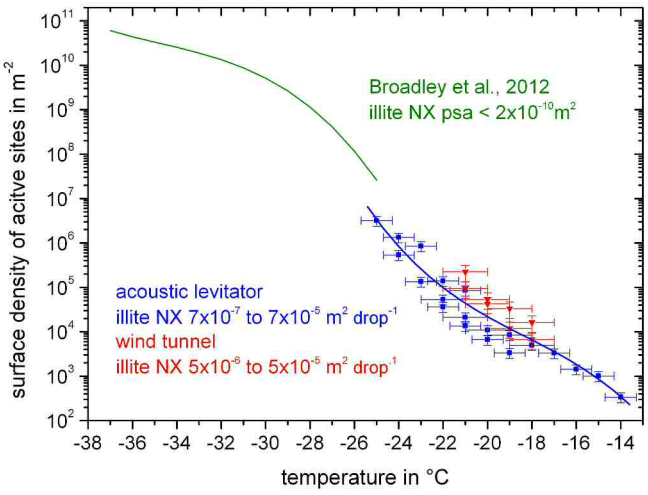


Figure 10: Surface densities of active sites as function of temperature for illite NX derived from present (shown in blue and red) and previous experiments (shown in green, from Broadley et al., 2012).